Spectroscopic Properties of a Self-Assembled Zinc Porphyrin Tetramer I. Steady State Optical Spectroscopy

Mikalai M. Yatskou,† Rob B. M. Koehorst, Harry Donker, and Tjeerd J. Schaafsma*

Laboratory of Molecular Physics, Department of Agrotechnology and Food Sciences, Wageningen University, Dreijenlaan 3, 6703 HA Wageningen, The Netherlands

Received: January 31, 2001; In Final Form: September 26, 2001

Aggregation of zinc mono-(4-pyridyl)-triphenylporphyrin (ZnPyP) in toluene and polystyrene/toluene mixtures has been investigated by steady-state optical spectroscopy. The Q-band absorption spectra, as well as the fluorescence spectra, show a temperature-dependent red shift as a result of ligation of the porphyrin zinc center. The smallest aggregate that can account for the optical spectra and their concentration dependence is a symmetrical tetramer in which each zinc atom is ligated to a pyridyl substituent of a neighboring porphyrin molecule. The Soret band shows a splitting, which can be explained by applying simple exciton theory to the tetramer. The equilibrium constant and thermodynamic parameters for the monomer−tetramer equilibrium have been determined as $K = (6.2 \pm 0.8) \times 10^{13}$ M^{-3}, $\Delta H = -40 \pm 2$ kCalM^{-1}, $\Delta S = -150 \pm 10$ Cal$K^{-1}M^{-1}$, in agreement with tetramer formation.

Introduction

Thin porphyrin films have been widely studied by optical spectroscopy for several reasons, one of them being their potential application in organic solar cells.[1−3] Photovoltaic cells have been constructed using two photoactive porphyrin layers acting as an electron donor and -acceptor, respectively.[4−6] The efficiency of these cells may be improved by making use of a light-collecting antenna transferring the excitation energy to the photoactive region of the cell, where charge separation takes place.

As in natural photosynthetic antenna complexes,[7−9] the efficiency of energy transfer relative to other photophysical processes in porphyrin complexes is expected to depend on the relative position and orientation of the porphyrins involved. Various porphyrin assemblies, both covalently as well as non-covalently bound, have been studied to obtain a better understanding of their photophysical properties, including internal energy transfer.[10−14] Although much progress has been made in understanding the excited-state kinetics in these porphyrin assemblies, the current understanding of the steady state and time-dependent properties of their excited state(s) is still incomplete.

This paper (I) reports the steady-state absorption- and fluorescence properties of a model system of a self-assembled symmetric porphyrin tetramer in toluene solution, using zinc mono (4-pyridyl)-triphenylporphyrin (ZnPyP, Figure 1) as a good candidate for self-assembled aggregates.[15−17] The ground-state structure of the tetramer cannot be determined from ^{1}H NMR ring current shifts[16,18−20] due the low solubility of the tetramer in toluene, and therefore has been calculated using a Chem-X program.[21] The thermodynamic parameters of the tetramer ground state are reported, whereas its excited-state properties are explained by simple exciton theory. The subsequent paper (II) presents the quantitative kinetics of the tetramer excited state using time-resolved fluorescence spectroscopy and anisotropy measurements. Both papers are part of a program, starting with a description of the photophysical processes in a well-defined porphyrin aggregate, to elucidate these processes in more complicated disordered and ordered solid porphyrin films, which may, for instance, serve as light-collecting antenna's in organic solar cells.

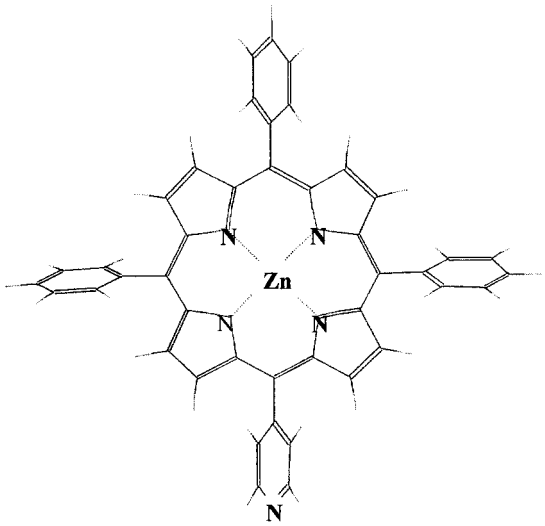

Figure 1. Structure of zinc mono-(4-pyridyl)-triphenylporphyrin.

In the experiments reported in this and the following paper, II, a solution of zinc tetraphenylporphyrin (ZnP) in dry toluene and in toluene/pyridine 1:10 v/v is used as a reference for the nonligated and ligated species, respectively. For the same reasons as mentioned before, similar studies as reported in this work have been carried out on a number of other tetra-phenyl-porphyrin derivatives including zinc tetra-(octylphenyl)-porphyrin (ZnTOPP).[22]

* To whom correspondence should be addressed. Tel: +31-317482044. Fax: + 31-317482725. E-mail: Tjeerd.Schaafsma@mac.mf.wau.nl.

† On leave from Department of Systems Analysis, Belarusian State University, 4, F. Scoryna Ave., Minsk, 220050, Belarus.

10.1021/jp010410p CCC: $20.00
Published on Web 11/30/2001

Experimental Section

Chemicals. Meso-tetraphenylporphyrin free base (H_2P) and a derivative with one meso-phenyl group substituted by a meso-(4-pyridyl) group, mono(4-pyridyl)-triphenylporphyrin free base (H_2PyP), were synthesized from pyrrole and benzaldehyde, and from pyrrole and a mixture of benzaldehyde and 4-pyridinecarbaldehyde, respectively, by standard procedures.[23] Zinc was inserted into the free base by refluxing a solution in dimethylformamide (DMF) in the presence of excess zinc(II)chloride[24] yielding ZnP and ZnPyP, respectively. The zinc porphyrins were purified by chromatography over silica gel (Merck) with chloroform (Merck, p.a.) as the eluent. The porphyrins were estimated to be >99% pure by thin-layer chromatography, absorption- and fluorescence spectroscopy. All reagents (Merck) were synthetic grade.

For optical measurements solutions were prepared in toluene (Merck, p.a.) after drying with sodium wire and storing over molecular sieve. Anhydrous pyridine (Aldrich) was used without additional drying or purification. For measurements of the steady-state fluorescence polarization anisotropy, the porphyrins were dissolved in viscous solutions of polystyrene (PS) in toluene (further denoted as PS/Tol). The latter solvent is more viscous than toluene and was used to distinguish between diffusional rotation and intramolecular energy transfer through steady state (Part I) and time-resolved fluorescence anisotropy measurements (Part II). All solvents used were p.a. grade, unless stated otherwise.

Steady-State Absorption and Fluorescence Measurements. A Cary 5E spectrophotometer and a Perkin-Elmer LS5 fluorimeter or a Fluorolog 3−22 Jobin Yvon spectrophotometer were used to record the electronic absorption- and fluorescence spectra. The Fluorolog spectrophotometer was equipped with two electronically actuated Glann−Thompson UV polarizers (Model 1008 Dual Auto Polarizer) to measure the steady-state anisotropy spectra. To study the effect of pyridine ligation, absorption − and fluorescence spectra were recorded of ≈22 and 16 μM ZnP solutions in neat toluene and in toluene/0.1 mM pyridine, respectively. Complexation of ZnPyP via intermolecular ligation of the zinc center of one porphyrin to a pyridyl substituent of a neighboring porphyrin was studied by measuring the absorption- and fluorescence spectra of 2.2−80 μM solutions in toluene over a 10−55 °C temperature range. Steady-state absorption- and fluorescence anisotropy spectra of ZnPyP in PS/Tol were recorded to study energy transfer processes within an aggregate.

Results

Temperature-dependent absorption spectra are shown in Figure 2 for solutions of (A): ≈22 μM ZnP in toluene, (B): ≈16 μM ZnP in toluene/0.1 mM pyridine, and (C): ≈40 μM ZnPyP in toluene. All spectra show similar absorption spectra at 55 °C, with maxima at 550 and 595 nm for the Q(1,0) and Q(0,0) bands, respectively, and at 423 nm for the Soret band. However, the absorption spectra of (A), (B), and (C) change differently with decreasing temperature. Decreasing the temperature from 55 to 10 °C results for (A) in only small changes of the absorption spectrum (Figure 2A), which may be due to ligation of ZnP with a trace amount of water still present in toluene despite drying on sodium wire.[25,26] For the same temperature range, the maxima of the Soret and Q(1,0), Q(0,0) absorption bands of (B) shift from 423 to 428 nm, from 550 to 561 nm, and from 589 to 601 nm, respectively (Figure 2B), whereas for (C) shifts were found from 550 to 560 nm and 589 to 604 nm for the Q(1,0) and Q(0,0) bands, respectively. At 10 °C, the Soret band is split into two components, of which one is red-shifted from 422 to 430 nm and the other is practically not shifted with respect to the monomer wavelength of 423 nm at 55 °C.

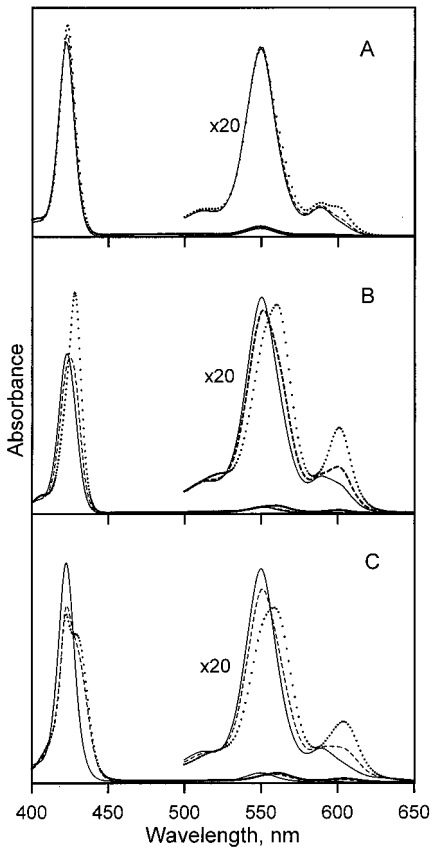

Figure 2. Effect of temperature on the absorption spectrum of (A) a ≈22 μM solution of ZnTPP in toluene, (B) a ≈16 μM solution of ZnTPP in a toluene/0.1 mM pyridine mixture, (C) a ≈40 μM solution of ZnPyP in toluene. Solid line: 55 °C; broken line: 35 °C; dotted line: 10 °C.

Fluorescence spectra of the same porphyrin samples at 10 and 55 °C are presented in Figure 3A−C. All spectra were recorded using excitation at the maximum of the Q(1,0) band. At 10 °C the fluorescence spectrum of (B) is red-shifted with respect to that of (A) (Figure 3A,B) and the intensity of the Q(0,0) band is higher than that of Q(0,1) typical for ligated metalloporphyrins.[27] For (C) at 10 °C (Figure 3C) the fluorescence spectrum looks similar to that of (B), but somewhat less resolved.

Steady-state fluorescence anisotropy spectra of ≈16 μM ZnP and the same concentration of ZnPyP in PS/Tol at 10 °C are presented in Figure 4A,B. The steady-state anisotropy spectrum of ZnP (Figure 4A) varies around a mean value of 0.1. The fluorescence anisotropy spectrum of ZnPyP (Figure 4B), which on the average has a lower amplitude than that of ZnP, has two minima, i.e., at 625 and 675 nm, and two maxima at 600 and 650 nm.

Discussion

The changes observed for the Soret- and Q-bands, presented in Figure 2B, are attributed to ligation of the metal center of ZnP to pyridine at 10 °C. From the shifts in both the Q and the Soret bands, we can conclude that at 10 °C ligation of ZnP with pyridine is almost complete,[28] whereas at 55 °C the equilibrium constant K for the equilibrium ZnPyP + L =

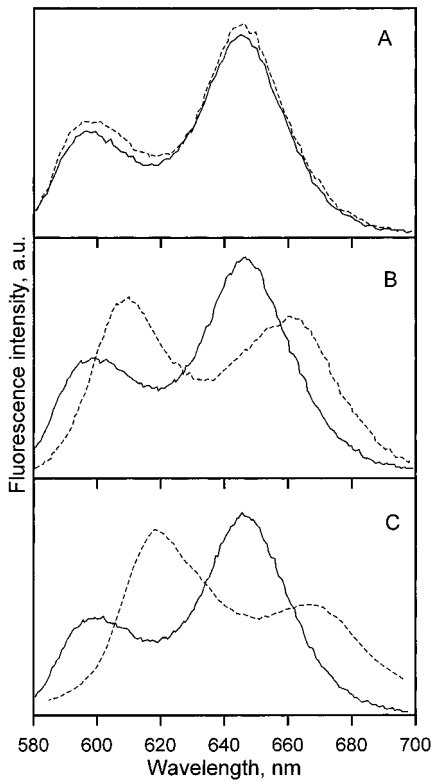

Figure 3. Effect of temperature on the fluorescence spectrum of (A) a ≈22 μM solution of ZnTPP in toluene, (B) a ≈16 μM solution of ZnTPP in a toluene/0.1 mM pyridine mixture, (C) a ≈40 μM solution of ZnPyP in toluene. Solid line: 55 °C; broken line: 10 °C. Excitation of all samples at the Q(1,0) maximum.

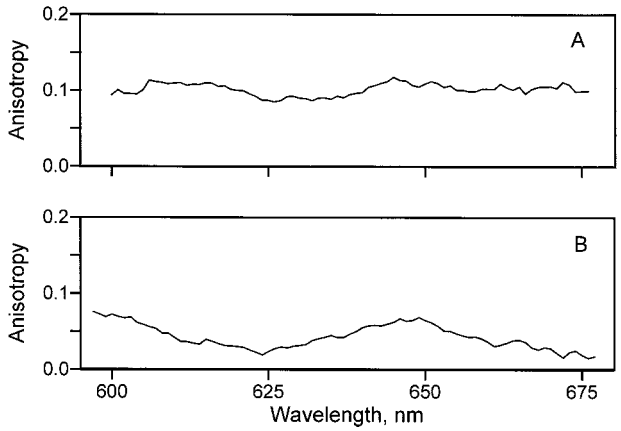

Figure 4. Steady-state anisotropy detected at 10 °C of (A) ≈16 μM ZnTPP; (B) ≈16 μM ZnPyP both in PS/Tol. Excitation at the Q(1,0) maximum.

ZnPyP·L is much smaller. With the coordinating ligand covalently linked to the porphyrin as for ZnPyP, a decrease of temperature of the solution is expected to result in porphyrin complexation via zinc-pyridyl ligation. Indeed, we observe Q-band shifts in the absorption spectrum upon a 55 to 10 °C temperature decrease (Figure 2C).[16,25] The Q-bands shifts are very similar to those in Figure 2B, and can therefore be ascribed to a high percentage of the ligated zinc porphyrin at 10 °C. Previously, the Soret band splitting was not observed for the same compound in $CHC1_3$[16] or just reported to be broadened[3] at 25 °C for toluene and CH_2C1_2 as a solvent. The split Soret band observed at 10 °C might suggest that only half of the ZnPyP molecules are internally ligated in agreement with a

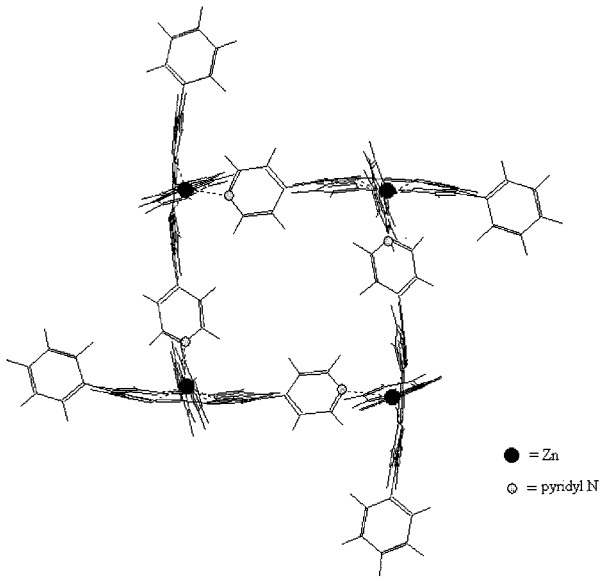

Figure 5. ZnPyP tetramer structure, calculated by the Chem X program.

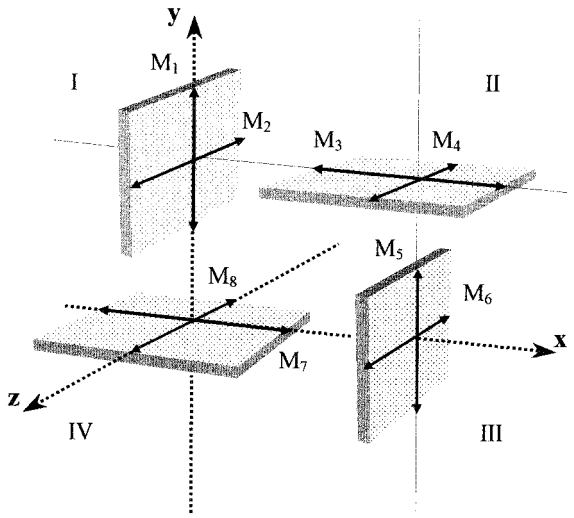

Figure 6. Structural arrangements of the transition moments (M_i), numbered i = 1,....8 in the ZnPyP tetramer. The porphyrin monomers in the aggregate are numbered I − IV.

dimer model as previously proposed,[3] but contradicting the observation that the entire Q-band is shifted. A polymeric structure for ZnPyP in $CHC1_3$ at concentrations up to 10 mM[16] is unlikely to explain our results in view of the low concentration (≈40 μM) which we have used. A symmetrical tetramer (Figure 5) in which each zinc atom is ligated to a pyridyl substituent of one of the neighboring porphyrin molecules is the smallest complex, which can account for the shift of the entire Q-band. The formation of a tetrameric complex also explains the splitting of the Soret band, invoking simple dipole−dipole excitonic interactions[29−31] in the S_2-state between four mutually perpendicular porphyrin molecules. The tetramer geometry is assumed to have C_{4h} symmetry (Figure 6).

The ground-state wave function of the tetramer is

$$\Psi_g = \psi_I\psi_{II}\psi_{III}\psi_{IV} \qquad (1)$$

where ψ_I, ψ_{II}, ψ_{III}, and ψ_{IV} are the ground-state wave functions of molecules numbered by I, II, III, and IV, respectively. The wave function for molecule I to be excited with a transition

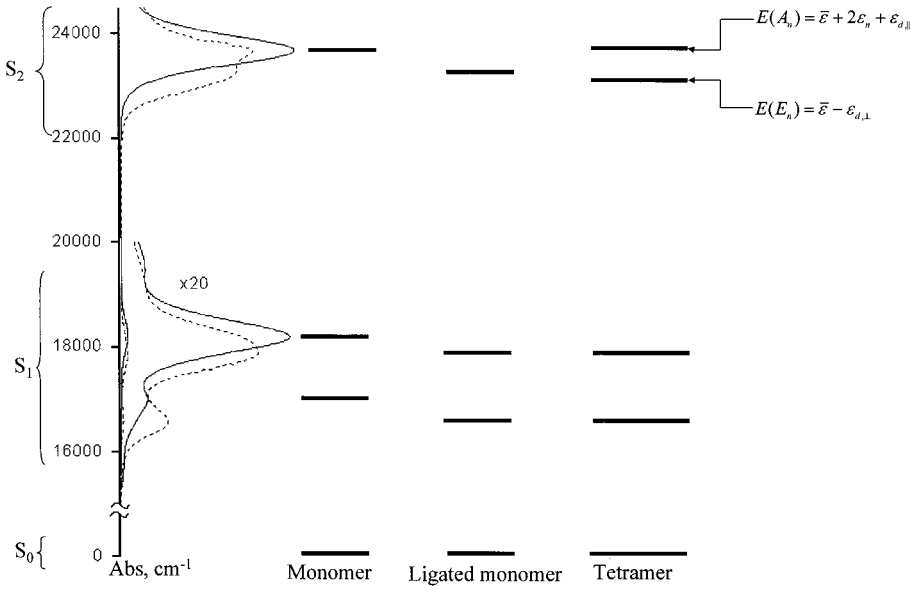

Figure 7. Tetramer energy level scheme, calculated using the exciton model (see text), and relative nonligated and ligated monomer energy levels.

dipole moment M_u either parallel ($u = \|$) or perpendicular ($u = \perp$) to the 4-fold axis (z, Figure 6) can then be written as

$$\Psi_{I,u} = \psi^*_{I,u}\psi_{II}\psi_{III}\psi_{IV}(u = \|, \perp) \tag{2}$$

and similarly for excitations localized on molecules II, III, and IV.

The excitonic wave functions resulting from a coupling V between these localized states have the general form

$$|k,u\rangle = \frac{1}{2}\sum_{j=I}^{IV} \exp(2\pi kji/4)\Psi_{j,u} \tag{3}$$

The eight possible states with $k = 0, \pm 1, 2$; $u = \|, \perp$ span the irreducible representations of the group C_{4h}. Of these only the state $|0,\|\rangle$ (A_u) and the 2-fold degenerate state $|\pm 1,\perp\rangle$ (E_u) are connected by electric-dipole-allowed transitions to the A_g ground state Ψ_g.

The wave functions of these states are

$$|0,\|\rangle = \frac{1}{2}(\Psi_{I,z} + \Psi_{II,z} + \Psi_{III,z} + \Psi_{IV,z})(A_u)$$

$$|1,x\rangle = 2^{-1/2}(\Psi_{II,\perp} - \Psi_{IV,\perp}); \; |1,y\rangle = 2^{-1/2}(\Psi_{I,\perp} - \Psi_{III,\perp})(E_u) \tag{4}$$

From eqs 2 and 4, it follows by inspection of Figure 6 that the energies and transition dipole moments of the allowed transitions are

$$E(A_n) = \bar{\epsilon} + 2\epsilon_n + \epsilon_{d,\|} \qquad M_\| = 2M$$

$$E(E_n) = \bar{\epsilon} - \epsilon_{d,\perp} \qquad M_x = M_y = \sqrt{2}M \tag{5}$$

where $\bar{\epsilon}$ is the energy of a locally excited-state plus the energy change of the constituents of the tetramer due to this excitation, ϵ_n (>0) is the coupling energy between the transition dipoles on neighboring molecules, e.g., $\epsilon_n = \langle\Psi_{I,\|}|V|\Psi_{II,\|}\rangle = \langle\Psi_{III,\|}|V|\Psi_{IV,\|}\rangle$, $\epsilon_{d,\|}$ is the coupling energy between molecules at the opposite sides of the tetramer, e.g., $\epsilon_{d,\perp} = \langle\Psi_{I,\perp}|V|\Psi_{III,\perp}\rangle$, $\epsilon_{d,\|} = \langle\Psi_{I,\|}|V|\Psi_{III,\|}\rangle$, and V is the intermolecular perturbation potential. In the present instance ϵ_n, $\epsilon_{d,\|}$, and $\epsilon_{d,\perp}$ are all positive.

Now we calculate the energy splitting ΔE between the two allowed transitions. From the optical spectrum of the ZnPyP monomer in toluene,[32] the dipole strength of the Soret band is calculated to be 9.5 ± 0.5 D. From the tetramer structure in a vacuum, calculated using the Chem-X program the center-to-center distances are found to be $\sim$10 Å for nearest neighbor porphyrins and $\sim$14 Å for the next nearest neighbor ones.

Using the point-dipole point-dipole approximation for V and the relative phases of the transition moments consistent with the 4-fold symmetry as indicated by the arrows in Figure 6, the coupling energies are calculated to be $\epsilon_n = 190 \pm 20$ cm^{-1}, $\epsilon_{d,\|} = 2\epsilon_{d,\perp} = 64 \pm 8$ cm^{-1}. The energy splitting ΔE between the two allowed transitions of the tetramer is calculated to be $\sim$480 $\pm$ 50 cm^{-1}, in good agreement with the experimental splitting $\sim$440 cm^{-1}. The calculated relative energy levels and transitions for the monomer, the ligated monomer, and the tetramer dipole arrangement are shown in Figure 7. According to the exciton model the component of the Soret band, which is red shifted wrt the nonligated monomer position, results from a superposition of two transition dipole−dipole interactions, i.e., M_1/M_5 and M_3/M_7. (Note that the transition moments are labeled by Arabic numbers, and the porphyrin monomers by Roman numbers). The band is 32 ± 4 cm^{-1} red-shifted wrt the position of the ligated monomer, too small a shift to be resolved in the absorption spectrum. In view of the discussion above, the component which is unshifted wrt the nonligated monomer position, is the result of excitonic interaction between four parallel transition dipole moments (M_2, M_4, M_6, and M_8) with the same directions. This band is significantly blue-shifted ($\Delta E \approx 440$ cm^{-1}) wrt the position of the ligated monomer. The total calculated dipole strengths are in agreement with those calculated from the experimental splitting of the Soret bands. The red-shift of the Q-bands only results from axial ligation of the zinc porphyrins because exciton interaction between the S_1 states is negligibly small due to the much smaller transition moments involved. It is important to note that application of the extended dipole−dipole model[33] does not significantly change the above-mentioned conclusions and changes the results of calculations with less than 10%.

The isosbestic points at 560 and 580 nm in the absorption spectra of Figure 2C indicate a shift in the equilibrium between two and only two species absorbing at different wavelengths at constant total concentration. The 2.2 μM ZnPyP spectrum measured at 55 °C, and the 80 μM ZnPyP spectrum measured at 15 °C can be assigned to the nonligated and the ligated molecules, respectively (In this context, ligated ZnPyP monomer refers to the absorption spectrum of 80 μM ZnPyP recorded at 15 °C). This conclusion is supported by the observation that the fluorescence spectra for the above two concentrations and temperatures are identical by exciting at λ = 415, 420, 425,-430, and 435 nm. This implies that the spectra at an arbitrary, intermediate concentration can be described as a linear combination of the spectra of the ligated and nonligated species.

For a given total concentration $C_{tot} = C_{ZnPyP}(T) + C_{ZnPyP\cdot L}(T)$ of the porphyrin in solution the concentration of nonligated and ligated entities at different temperatures can then be determined by applying Lambert−Beer's law to the absorption spectrum. If $A_{tot}(\lambda,T)$ is the total absorbance at a temperature T (°C) and wavelength λ (nm) then

$$A_{tot}(\lambda,T) = [C_{ZnPyP}(T)\cdot\epsilon_{ZnPyP}(\lambda) + C_{ZnPyP\cdot L}(T)\cdot\epsilon_{ZnPyP\cdot L}(\lambda)]\cdot\tilde{l} \quad (6)$$

where ϵ_{ZnPyP} and $\epsilon_{ZnPyP\cdot L}$ are the molar extinction coefficients ($lM^{-1}cm^{-1}$) for the nonligated and ligated molecules, assumed constant over the experimental temperature range, and $\tilde{l} = 1$ cm is the cuvette path-length. (For reasons of simplicity and because $\tilde{l} = 1$ cm in our measurements we omit $\tilde{l}$ from further consideration). With absorbance data taken from the absorption spectra of the dilute and concentrated solutions measured at 55 and 15 °C, respectively, eq 6 can be rewritten as

$$A^T_{tot}(\lambda,T) = C^T_{ZnP}\cdot\frac{A_{2.2\,\mu M}(\lambda,55\,°C)\cdot\epsilon_{ZnPyP}(550\text{ nm})}{A_{2.2\,\mu M}(550\text{ nm},55\,°C)} + C_{ZnPyP\cdot L}(T)\cdot\frac{A_{80\,\mu M}(\lambda,15\,°C)\cdot\epsilon_{ZnPyP\cdot L}(560\text{ nm})}{A_{80\,\mu M}(560\text{ nm},15\,°C)} \quad (7)$$

Thus, from eq 7 the concentrations $C_{ZnPyP}(T)$, $C_{ZnPyP\cdot L}(T)$ of nonligated and ligated porphyrins can now be calculated using $\epsilon_{ZnP}(550\text{ nm}) = 22\,000\ lM^{-1}cm^{-1}$ and $\epsilon_{ZnP\cdot L}(560\text{ nm}) = 20\,000\ lM^{-1}cm^{-1}$.[3] The results calculated for the three different ZnPyP concentrations are plotted in Figure 8.

If there were noncyclic complexes (e.g., dimers, trimers, or oligomers) in our samples unidirectional energy transfer is expected to occur from an excited, nonligated porphyrin to a neighboring, ligated one because of considerable overlap between the fluorescence- and absorption spectra of nonligated- and ligated ZnPyP. Consequently, the presence of nonligated monomers in these structures should result in a decrease of the fluorescence yield of the nonligated species and a simultaneous increase of the yield of the ligated species with decreasing temperature. Such a temperature dependence of the fluorescence yield has not been found for solutions at intermediate concentrations (C_{tot} = 22 μM, excitation at 550 nm) when this is simulated in the same way as the absorption spectra, by the summation

$$I_{tot}(\lambda,T) = I_{ZnPyP}(\lambda,T) + I_{ZnPyP\cdot L}(\lambda,T) \quad (8)$$

(Note that for the 2.2 μM solution the 55 °C fluorescence spectrum completely originates from nonligated monomers, and for the 80 μM solution from the ligated species).

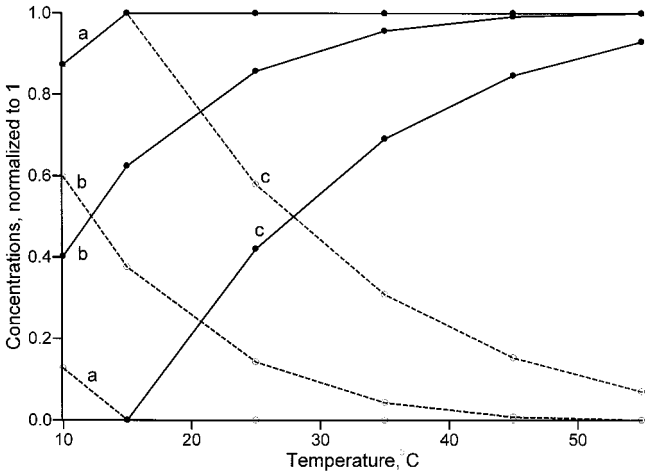

Figure 8. Concentrations of the nonligated monomers $\tilde{C}_{ZnPyP}$(solid curves) and ligated monomers $\tilde{C}_{ZnPyP\cdot L}$(broken lines) of (set a) 2.2 μM, (set b) 22 μM, and (set c) 80 μM ZnPyP vs temperature. $\tilde{C}_{ZnPyP} + \tilde{C}_{ZnPyP\cdot L}$ is normalized to 1.

Making the reasonable assumption that the fluorescence intensity of each species varies linearly with its concentration we then have the following analogue to eq 7

$$I_{tot}(\lambda,T) = [C_{ZnPyP}(T)/2.2\times10^{-6}]I_{2.2\,\mu M}(\lambda,55\,°C) + [C_{ZnPyP\cdot L}(T)/8.0\times10^{-5}]I_{8.0\,\mu M}(\lambda,10\,°C) \quad (9)$$

When analyzing the experimental fluorescence spectra using eq 9, we conclude to the same relative contributions of ZnPyP and ZnPyP·L as derived from the temperature dependence of the absorption spectra. This result is in agreement with the proposed tetramer formation and contradicts a model that includes formation of noncyclic structures.

The steady-state fluorescence polarization anisotropy of ZnPyP at the maxima of the Q-transitions is at most half that of the ZnP spectrum (Figure 4A). Using the Perrin equation for the steady-state anisotropy

$$r = \beta_0/(1 + (\tau/\phi)) \quad (10)$$

with β_0 the magnitude of the initial anisotropy, τ the fluorescence lifetime, and ϕ the effective rotational volume of the molecule, the value of the steady-state anisotropy can be approximated as $r = \beta_0$. As can be seen from Figure 4 β_0 is ~0.1 for monomers and $\beta_0 \sim 0.025$ for tetramers at the maxima of the Q-transitions. Note that for zinc porphyrins in viscous PS/Tol solution $\tau/\phi \ll 1$ and for a cyclic symmetrical porphyrin tetramer β_0 is expected to be 0.025 (see Part II). The decrease of the initial anisotropy is an indication of an additional depolarization channel in the tetramer by one or more energy transfer processes within the tetramer. The increase of the steady-state anisotropy around 600 and 650 nm indicates the presence of a fraction of nonligated monomers. The effects of energy transfer on the time dependence of the fluorescence anisotropy are analyzed in more detail in Part II.

The changes in the absorption spectra resulting from tetramer formation may be utilized to quantitatively study the equilibrium reaction by the noncalorimetric thermodynamic method.[34] Although this method has limited accuracy it provides an additional argument for the proposed monomer-tetramer equi-

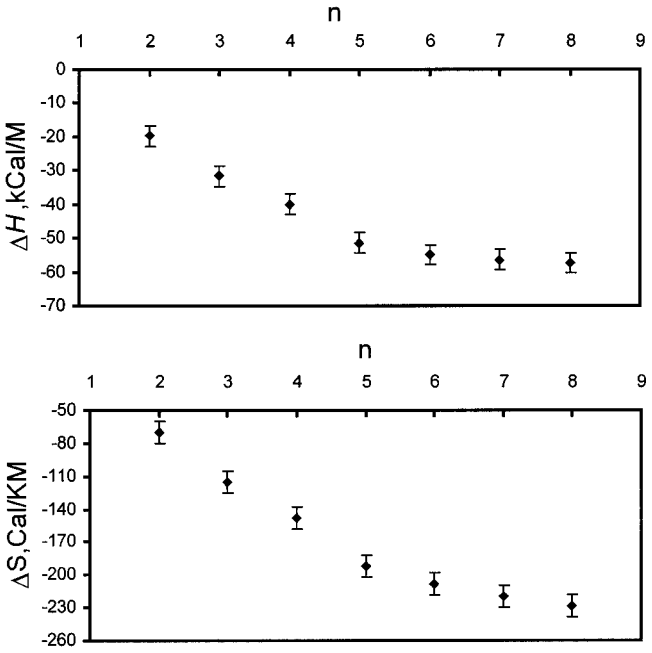

Figure 9. Enthalpy ΔH and entropy ΔS for the equilibrium between n molecules ZnPyP and the aggregate $(ZnPyP)_n$.

librium. Generally, the equilibrium constant $K[_{ZnPyPn}]$ for the reactions: $n\cdot[ZnPyP] = [ZnPyP]_n$ obeys the equation[34]

$$K[_{ZnPyP}]_n = [ZnPyP]_n/[ZnPyP]^n \qquad (11)$$

where [ZnPyP] and $[ZnPyP]_n$ are the molar concentrations of the monomer and an aggregate of n ligated molecules, respectively. Taking the monomer concentration of nonligated and ligated porphyrins from Figure 8 and using eq 11, the enthalpy ΔH and entropy ΔS with n can be calculated from the slopes of the van't Hoff plots.[34] Figure 9 presents ΔH and ΔS for aggregates formed by $n = 2,...8$ ligated molecules. The values $n = 2,3,7,8$ need not be considered as their van't Hoff plots are distinctly nonlinear, which would imply an equilibrium between more than two species, contradicting the finding of an isosbestic point of the optical spectra. Also, ΔS values do not change much for $n \geq 6$, which indicates that large aggregates ($n \geq 6$) can also be rejected, leaving aggregates with $n = 4$ and 5 to be considered. The smallest aggregate has $n = 4$ which agrees with the result of the calculation of the excitonic splitting of the Soret band and with the 0.025 value of initial anisotropy derived from the steady-state fluorescence polarization anisotropy spectrum of ZnPyP. For tetramers involved in the reaction, $K[_{ZnPyPn}]$, ΔH, and ΔS are calculated to be $6.2 \pm 0.8\ 10^{13}\ M^{-3}$, -40 ± 2 $kCalM^{-1}$, and $-150 \pm 10\ CalK^{-1}M^{-1}$, respectively. The van't Hoff plot is shown in Figure 10. ΔH for insertion of one ZnPyP molecule into the tetrameric complex is $-10\ kcalM^{-1}$ in good agreement with values calculated for the ZnP/pyridine equilibrium.[35,36] ΔS is almost one order larger than for ZnP ligated to pyridine,[35,36] that also supports the formation of a relatively large closed structure.

Conclusions

This work demonstrates that the effects of lowering the temperature or increasing the concentration of a ZnPyP/toluene solution on the absorption- and fluorescence spectra are the result of porphyrin aggregation; the shifts, found in both the Q-band region of the absorption spectrum and in the fluorescence spectrum, can be ascribed to coordination of the metal center of one ZnPyP molecule to the pyridyl substituent of a second, neighboring molecule. Excitonic interactions can be neglected for the S_1 state; the splitting of the Soret band in the absorption spectrum can be explained by an excitonic interaction in the S_2-state between four perpendicularly oriented ZnPyP molecules in a structure in which each zinc atom is ligated to a pyridyl substituent of a neighboring molecule; other structures, involving a different number of porphyrins in the aggregate or different geometries cannot completely be excluded, but are less likely.

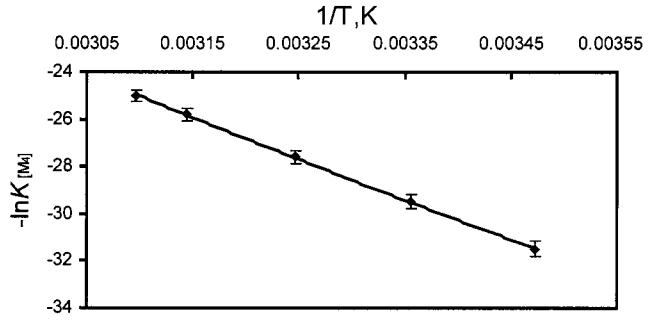

Figure 10. Van't Hoff plot for the equilibrium $4[ZnPyP] = [ZnPyP]_4$, with [ZnPyP] and $[ZnPyP]_4$ the molar concentrations of monomers and tetramers, respectively.

A symmetrical tetramer is the smallest complex that can account for all of the observed shifts in the optical spectra; the estimated thermodynamic parameters are in agreement with those expected for a tetramer.

The above conclusions are supported and extended in part II of this paper describing time-resolved fluorescence- and fluorescence anisotropy measurements.

References and Notes

(1) Schaafsma, T. J. *Sol. Energy Mater. Sol. Cells* **1995**, *38*, 349.
(2) Leray, I.; Verniéres, M. C.; Pansu, R.; Bied-Charreton, C.; Faure, J. *Thin Solid Films* **1997**, *303*, 295.
(3) Takahashi, K.; Komura, T.; Imanaga, H. *Bull. Chem. Soc. Jpn.* **1989**, *62*, 386.
(4) Savenije, T. J.; Koehorst, R. B. M.; Schaafsma, T. J. *Chem. Phys. Lett.* **1995**, *244*, 363.
(5) Günster, S.; Siebentritt, S.; Meissner, D. *Mol. Cryst. Liq. Cryst. A* **1993**, *230*, 351.
(6) Wöhrle, D.; Tennigkeit, B.; Elbe, J.; Kreienhop, L.; Schnurpfeil, G. *Mol. Cryst. Liq. Cryst. A* **1993**, *230*, 221.
(7) Larkum, A. W. D.; Barrett, J. *Adv. Bot. Res.* **1983**, *10*, 1.
(8) Scheer, H.; Siegried, S.; de Gruyter, W. *Photosynthetic Light-Harvesting Systems*; Springer: Berlin, 1988.
(9) Karrasch, S.; Bullough, P. A.; Ghosh, R. *EMBO J.* **1995**, *14*, 631.
(10) Prodi, A.; Indelli, M. T.; Kleverlaan, C. J.; Scandola, F.; Alessio, E.; Gianferrara, T.; Marzilli, L. G. *Chem. Eur. J.* **1999**, *5*, 2668.
(11) Rubtsov, I. V.; Kobuke, Y.; Miyaji, H.; Yoshihara, K. *Chem. Phys. Lett.* **1999**, *308*, 323.
(12) Lawrence, D.; Jiang, I.; Levett, M. *Chem. Rev.* **1995**, *95*, 2229.
(13) Li, F.; Gentemann, S.; Kalsbeck, W. A.; Seth, J.; Lindsey, J. S.; Holten, D.; Bocian, D. F. *J. Mater. Chem.* **1997**, *7*, 1245.
(14) van Patten, P. J.; Shreve, A. P.; Lindsey, J. S.; Donohoe, R. J. *J. Phys. Chem. B* **1998**, *102*, 4209.
(15) Alessio, E.; Gremia, S.; Mestroni, S.; Iengo, E.; Srnova, I.; Slof, M. *Inorg. Chem.* **1999**, *38*, 869.
(16) Fleiscer, E. B.; Shachter, A. M. *Inorg. Chem.* **1991**, *30*, 3763.
(17) Shachter, A. M.; Fleiscer, E. B.; Haltiwanger, R. C. *J. Chem. Soc. Chem. Commun.* **1988**, 960.
(18) Abraham, R. J. *J. Mol. Phys.* **1961**, *4*, 145.
(19) Hofstra, U.; Koehorst, R. B. M.; Schaafsma, T. J. *Magn. Reson. Chem.* **1987**, *25*, 1069.
(20) Koehorst, R. B. M.; Hofstra, U.; Schaafsma, T. J. *Magn. Reson. Chem.* **1988**, *26*, 167.
(21) *Chem-X*; Chemical Design Ltd: Oxon, England, 1993.

(22) Donker, H.; Koehorst, R. B. M.; van Hoek, A.; van Schaik, W.; Yatskou, M. M.; Schaafsma, T. J. *J. Phys. Chem. B*, submitted.
(23) Adler, A. D.; Longo, F. R.; Finarelli, J. D.; Goldmacher, J.; Assour, J.; Korsakoff, L. *J. Organic Chem.* **1967**, *32*, 476.
(24) Adler, A. D.; Longo, F. R.; Kampas, F.; Kim, J. *J. Inorg. Nucl. Chem.* **1970**, *32*, 2443.
(25) Nardo; J. V.; Dawson, J. H. *Inorg. Chem. Acta* **1986**, *123*, 9.
(26) Datta-Gupta, N.; Malakar, D.; Ramcharan, R. G. *J. Inorg. Nucl. Chem.* **1981**, *43*, 2079.
(27) Selensky, R.; Holten, D.; Windsor, M. W.; Paine, J. B., III.; Dolphin, D.; Gouterman, M.; Thomas, J. C. *Chem. Phys.* **1981**, *60*, 33.
(28) Humphry-Baker, R.; Kalyanasundaram, K. *J. Photochemistry* **1985**, *31*, 105.
(29) McRae, E. G.; Kasha, M. *J. Chem. Phys.* **1958**, *28*, 721.
(30) Kasha, M.; Rawls, H. R.; El-Bayoumi, M. A. *Pure Appl. Chem.* **1965**, *11*, 371.
(31) Stomphorst, R. G.; Koehorst, R. B. M.; van der Zwan, G.; Benthem, B.; Schaafsma, T. J. *J. Porph. Phthalocyanins* **1999**, *3*, 346.
(32) Michl, T.; Thulstrup, E. W. *Spectroscopy with Polarized Light*; VCH: New York, 1986.
(33) Czikklely, V.; Forsterling, H. D.; Kuhn, H. *Chem. Phys. Lett.* **1970**, *6*, 207.
(34) Atkins, P. W. *Physical Chemistry*; Oxford University Press: Oxford, 1998.
(35) Miller, J. R.; Dorought, G. D. *J. Am. Chem. Soc.* **1952**, *74*, 3977.
(36) Datta-Gupta, N.; Malakar, D.; Ramcharan, R. G.*J. Inorg. Nucl. Chem.* **1981**, *43*, 2079.